

SUSY Production From TeV Scale Blackhole at LHC

Andrew Chamblin,^{1,*} Fred Cooper,^{2,†} and Gouranga C. Nayak^{3,‡}

¹*Department of Physics, University of Louisville, Louisville, KY 40292, USA*

² *National Science Foundation, Arlington,*

VA 22230, USA and T-8, Theoretical Division,

Los Alamos National Laboratory, Los Alamos, NM 87545, USA

³ *C. N. Yang Institute for Theoretical Physics,*

Stony Brook University, SUNY, Stony Brook, NY 11794-3840, USA

(Dated: February 1, 2008)

Abstract

If the fundamental Planck scale is near a TeV, then we should expect to see TeV scale black holes at the LHC. Similarly, if the scale of supersymmetry breaking is sufficiently low, then we might expect to see light supersymmetric particles in the next generation of colliders. If the mass of the supersymmetric particle is of order a TeV and is comparable to the temperature of a typical TeV scale black hole, then such sparticles will be copiously produced via Hawking radiation: The black hole will act as a resonance for sparticles, among other things. In this paper we compared various signatures for SUSY production at LHC, and we contrasted the situation where the sparticles are produced directly via parton fusion processes with the situation where they are produced indirectly through black hole resonances. We found that black hole resonances provide a larger source for heavy mass SUSY (squark and gluino) production than the direct pQCD-SUSY production via parton fusion processes depending on the values of the Planck mass and blackhole mass. Hence black hole production at LHC may indirectly act as a dominant channel for SUSY production. We also found that the differential cross section $d\sigma/dp_t$ for SUSY production increases as a function of the p_t (up to p_t equal to about 1 TeV or more) of the SUSY particles (squarks and gluinos), which is in sharp contrast with the pQCD predictions where the differential cross section $d\sigma/dp_t$ decreases as p_t increases for high p_t about 1 TeV or higher. This is a feature for any particle emission from TeV scale blackhole as long as the temperature of the blackhole is very high (\sim TeV). Hence measurement of increase of $d\sigma/dp_t$ with p_t for p_t up to about 1 TeV or higher for final state particles might be a useful signature for blackhole production at LHC.

PACS numbers: PACS:

*Electronic address: chamblin@lns.mit.edu

[†]Electronic address: fcooper@nsf.gov

[‡]Electronic address: nayak@insti.physics.sunysb.edu

I. INTRODUCTION

It is now generally accepted that the scale of quantum gravity *could be* as low as a TeV [1]. Also, it is unknown if supersymmetry is manifested in nature, and if SUSY does exist it is unclear at what energy scale SUSY becomes manifest. Pragmatically, we can only search for black holes, extra dimensions and superpartners in whatever mass range is currently accessible to experiment. If we manage to detect *any* of these exotic phenomena, then we will be propelled into the twenty-first century, as our understanding of quantum gravity and perhaps even string theory is revolutionized. There are many discussions of graviton, radion and black hole production at LHC. If such processes occur they will probe TeV scale quantum gravity at the collider experiments [2, 3]. One of the most exciting aspects of this TeV scale gravity will be the production of black holes in particle accelerators. These ‘brane-world’ black holes will be our first window into the extra dimensions of space predicted by string theory, and required by the several brane-world scenarios that provide for a low energy Planck scale [4]. Using various approximations, in a number of recent papers people have studied the production of microscopic black holes in proton-proton (pp) and lead-lead (PbPb) collisions at LHC and cosmic ray events [5, 6, 7, 8, 9, 10, 11, 12, 13, 14, 15, 16, 17, 18, 19, 20, 21]. Typically, it only makes sense to say that a ‘black hole’ has formed at several times the Planck scale - anything smaller will dissolve into something known as string ball [22]. Thus, if the lightest supersymmetric particle (LSP) is sufficiently lighter than the black hole temperature, then we expect that such sparticles will be produced as the black hole evaporates through the Hawking process [23]. Naively, the lighter the LSP, and the larger the Planck scale then the more sparticles we expect to see produced through this process. However, as the Planck scale is increased the production cross section of the blackhole in pp collisions at LHC is decreased. Hence, SUSY production comes from two competitive effects as the Planck scale is increased: 1) the SUSY production from a single blackhole increases 2) the cross section for a single blackhole to be produced decreases. Similarly, if the SUSY scale is right near the Planck scale, then the rate for sparticle production through this channel is minimal. In this paper we perform a systematic analysis which contrasts SUSY (squark and gluino) production from direct pQCD-SUSY production processes with SUSY emission from a blackhole via Hawkins radiation at LHC. We find that squark and gluino production from a blackhole at LHC can be larger or smaller than direct squark and

gluino production from pQCD-SUSY processes depending on the value of the TeV scale Planck mass, the number of extra dimensions and the black hole mass. We find that as long as the temperature of the blackhole is of the order of a TeV, the squark and gluino production cross sections from the blackhole do not depend too much on the squark and gluino masses. On the otherhand the direct pQCD-SUSY production cross sections seriously depend on the masses of the squark and gluino, since in any massive particle production using pQCD calculations the cross section depends on the mass explicitly. This provides us with an important conclusion: If TeV scale blackholes are indeed formed at LHC, then one signature of this will be an unusually copious production of massive particles, which can not be formed through direct fusion processes. Hence if we observe very high rates of massive particle production at LHC, it might provide indirect evidence that TeV scale blackholes are being produced at LHC. We make a detailed analysis of this in this paper in the context of massive squark and gluino production. We also study the differential cross section for squark and gluino production both from the blackhole and from the pQCD-SUSY processes. One of the interesting results we find is that as long as the temperature of the blackhole is very high (~ 1 TeV) then the differential cross section $d\sigma/dp_t$ increases as p_t is increased (up to about p_t equal to 1 TeV or more). This is in sharp contrast to pQCD predictions where $d\sigma/dp_t$ decreases as p_t is increased when one is at high p_t . This is not only true for SUSY particles but also true for any particles emitted from a blackhole via Hawking radiation as long as the temperature of the black hole is high (\sim TeV). This is very interesting because if one experimentally observes at LHC that the $d\sigma/dp_t$ for final state particles increases as p_t is increased (up to about 1 TeV or higher) then it might provide a good signature for blackhole production at LHC. We make a detailed analysis of all these observations in this paper.

The paper is organized as follows: In section II we present the calculation of the differential and total cross sections for squark and gluino production at LHC in a typical MSSM scenario, where we take the gluino to be the LSP. In section III we present a computation for the rate of squark and gluino production from a blackhole via Hawking radiation. In section IV we present the results and a discussion.

II. SQUARK AND GLUINO PRODUCTION IN PP COLLISIONS AT LHC USING pQCD

Here we briefly discuss the SUSY (squark and gluino) production mechanism in quark and gluon fusion processes using pQCD methods applied to high energy hadronic collisions. The production channels for squarks ($\tilde{q}, \tilde{\bar{q}}$) and gluinos (\tilde{g}) in pp collisions at the leading order (LO) of the perturbative expansion are given by: $q\bar{q}$, $gg \rightarrow \tilde{q}\tilde{\bar{q}}$, $\tilde{g}\tilde{g}$, $q\bar{q} \rightarrow \tilde{q}\tilde{\bar{q}}$, $qg \rightarrow \tilde{q}\tilde{g}$ etc. The Feynman diagrams for these processes are shown in Fig. 1. For the production of squark pairs or squark–gluino pairs only one initial state contributes at lowest order. For squark–antisquark and gluino pairs both gluon–gluon and quark–antiquark initial states are included. The differential cross section in the lowest order is given by:

$$\frac{d\sigma}{dp_t^2 dy} = \frac{H}{s} \sum_{i,j=q,\bar{q},g} \int_{x_1^{min}}^1 dx_1 \left(-\frac{1}{x_1^2 t} \right) f_{i/A}(x_1, p_t^2) f_{j/B}(-\frac{x_1 ts}{x_1 s + u}, p_t^2) \times \sum |M|^2 \left(\frac{-x_1^2 ts}{x_1 s + u}, x_1 t, -\frac{x_1 tu}{x_1 s + u} \right) \quad (1)$$

where s is the total center of mass energy at hadronic level, $t = -\sqrt{s(p_t^2 + m^2)} e^y$ and $u = -\sqrt{s(p_t^2 + m^2)} e^{-y}$. The lower limit of the x_1 integration is given by $x_1^{min} = -u/s + t$. $f_{i/p}(x, Q^2)$ is the parton distribution function inside a proton with longitudinal momentum fraction x and factorization scale Q . $H = K_{ij}/16\pi$ with $K_{qq} = K_{q\bar{q}} = 1/36$, $K_{gg} = 1/256$ and $K_{qg} = 1/96$. The matrix element squares from partonic fusion processes at the Born level (see Fig-1) are given by [24]:

$$\begin{aligned} \sum |\mathcal{M}^B|^2 (q_i \bar{q}_j \rightarrow \tilde{q} \bar{\tilde{q}}) &= \delta_{ij} \left[32 n_f g_s^4 \frac{\hat{t}_q \hat{u}_q - m_{\tilde{q}}^2 \hat{s}}{\hat{s}^2} + 16 \hat{g}_s^4 \frac{\hat{t}_q \hat{u}_q - (m_{\tilde{q}}^2 - m_{\tilde{g}}^2) \hat{s}}{\hat{t}_g^2} \right. \\ &\quad \left. - 32/3 g_s^2 \hat{g}_s^2 \frac{\hat{t}_q \hat{u}_q - m_{\tilde{q}}^2 \hat{s}}{\hat{s} \hat{t}_g} \right] + (1 - \delta_{ij}) \left[16 \hat{g}_s^4 \frac{\hat{t}_q \hat{u}_q - (m_{\tilde{q}}^2 - m_{\tilde{g}}^2) \hat{s}}{\hat{t}_g^2} \right] \\ \sum |\mathcal{M}^B|^2 (gg \rightarrow \tilde{q} \bar{\tilde{q}}) &= 4 n_f g_s^4 \left[24 \left(1 - 2 \frac{\hat{t}_q \hat{u}_q}{\hat{s}^2} \right) - 8/3 \right] \left[1 - 2 \frac{\hat{s} m_{\tilde{q}}^2}{\hat{t}_q \hat{u}_q} \left(1 - \frac{\hat{s} m_{\tilde{q}}^2}{\hat{t}_q \hat{u}_q} \right) \right] \\ \sum |\mathcal{M}^B|^2 (q_i q_j \rightarrow \tilde{q} \tilde{q}) &= \delta_{ij} \left[8 \hat{g}_s^4 \left(\hat{t}_q \hat{u}_q - m_{\tilde{q}}^2 \hat{s} \right) \left(\frac{1}{\hat{t}_g^2} + \frac{1}{\hat{u}_g^2} \right) \right. \\ &\quad \left. + 16 \hat{g}_s^4 m_{\tilde{g}}^2 \hat{s} \left(\left(\frac{1}{\hat{t}_g^2} + \frac{1}{\hat{u}_g^2} \right) - 8/3 \frac{1}{\hat{t}_g \hat{u}_g} \right) \right] \\ &\quad + (1 - \delta_{ij}) \left[16 \hat{g}_s^4 \frac{\hat{t}_q \hat{u}_q - (m_{\tilde{q}}^2 - m_{\tilde{g}}^2) \hat{s}}{\hat{t}_g^2} \right] \end{aligned}$$

$$\begin{aligned}
\sum |\mathcal{M}^B|^2(q\bar{q} \rightarrow \tilde{g}\tilde{g}) &= 96g_s^4 \left[\frac{2m_{\tilde{g}}^2\hat{s} + \hat{t}_g^2 + \hat{u}_g^2}{\hat{s}^2} \right] \\
&\quad + 96g_s^2\hat{g}_s^2 \left[\frac{m_{\tilde{g}}^2\hat{s} + \hat{t}_g^2}{\hat{s}\hat{t}_q} + \frac{m_{\tilde{g}}^2\hat{s} + \hat{u}_g^2}{\hat{s}\hat{u}_q} \right] \\
&\quad + 2\hat{g}_s^4 \left[24 \left(\frac{\hat{t}_g^2}{\hat{t}_q^2} + \frac{\hat{u}_g^2}{\hat{u}_q^2} \right) + 8/3 \left(2 \frac{m_{\tilde{g}}^2\hat{s}}{\hat{t}_q\hat{u}_q} - \frac{\hat{t}_g^2}{\hat{t}_q^2} - \frac{\hat{u}_g^2}{\hat{u}_q^2} \right) \right] \\
\sum |\mathcal{M}^B|^2(gg \rightarrow \tilde{g}\tilde{g}) &= 576g_s^4 \left(1 - \frac{\hat{t}_g\hat{u}_g}{\hat{s}^2} \right) \left[\frac{\hat{s}^2}{\hat{t}_g\hat{u}_g} - 2 + 4 \frac{m_{\tilde{g}}^2\hat{s}}{\hat{t}_g\hat{u}_g} \left(1 - \frac{m_{\tilde{g}}^2\hat{s}}{\hat{t}_g\hat{u}_g} \right) \right] \\
\sum |\mathcal{M}^B|^2(qg \rightarrow \tilde{q}\tilde{g}) &= 2g_s^2\hat{g}_s^2 \left[24 \left(1 - 2 \frac{\hat{s}\hat{u}_q}{\hat{t}_g^2} \right) - 8/3 \right] \left[- \frac{\hat{t}_g}{\hat{s}} \right. \\
&\quad \left. + \frac{2(m_{\tilde{q}}^2 - m_{\tilde{g}}^2)\hat{t}_g}{\hat{s}\hat{u}_q} \left(1 + \frac{m_{\tilde{q}}^2}{\hat{u}_q} + \frac{m_{\tilde{g}}^2}{\hat{t}_g} \right) \right].
\end{aligned}$$

In the above equation the variables $\hat{t}_{q,g}$ ($\hat{u}_{q,g}$) are related to the Mandelstam variables \hat{t} (\hat{u}) by: \hat{t}_q (\hat{u}_q) = \hat{t} (\hat{u}) − $m_{\tilde{q}}^2$ and \hat{t}_g (\hat{u}_g) = \hat{t} (\hat{u}) − $m_{\tilde{g}}^2$ where $m_{\tilde{q}}$ ($m_{\tilde{g}}$) is the mass of the squark (gluino). g_s is the QCD gauge coupling (qqg) and \hat{g}_s is the Yukawa coupling ($q\tilde{q}\tilde{g}$). n_f is the number of flavors. In the above equations:

$$\hat{s} = -\frac{x_1^2ts}{x_1s+u} \quad \hat{t}_{g(q)} = x_1t \quad \hat{u}_{g(q)} = -\frac{x_1tu}{x_1s+u}. \quad (2)$$

The p_t distributions for squarks and gluinos at LHC are determined from the above formula by integrating over the rapidity:

$$\frac{d\sigma}{dp_t} = 2p_t \int_{-\cosh^{-1}(\frac{\sqrt{s}}{2(\sqrt{p_t^2+m^2})})}^{\cosh^{-1}(\frac{\sqrt{s}}{2(\sqrt{p_t^2+m^2})})} dy \frac{d\sigma}{dm_t^2 dy}. \quad (3)$$

Similarly, the rapidity distributions for squarks and gluinos produced at LHC are given by by integrating over p_t :

$$\frac{d\sigma}{dy} = \int_{m^2}^{s/4\cosh^2y} dm_t^2 \frac{d\sigma}{dm_t^2 dy}. \quad (4)$$

The total cross sections for squarks and gluinos produced at LHC are then given by:

$$\sigma^{pp \rightarrow \tilde{q}\tilde{q}(\tilde{g}\tilde{g})} = \Sigma_{i,j} \int_{4M^2/s} dx_1 \int_{4m^2/sx_1} dx_2 f_{i/p}(x_1, Q^2) f_{j/p}(x_2, Q^2) \sigma^{ij}(\hat{s}) \quad (5)$$

where σ^{ij} is the partonic level cross section for the collisions $ij \rightarrow \tilde{q}\tilde{q}(\tilde{g}\tilde{g})$ etc., where the indices i, j run over q, \bar{q} and g. The partonic level center of mass energy is related to the hadronic level center of mass energy by: $\hat{s} = x_1x_2s$. The partonic level squark and gluino production cross sections $\sigma^{ij}(\hat{s})$ can be obtained from the matrix element squares above and are given by:

$$\begin{aligned}
\sigma^B(q_i \bar{q}_j \rightarrow \tilde{q} \bar{\tilde{q}}) &= \delta_{ij} \frac{n_f \pi \alpha_s^2}{\hat{s}} \beta_{\tilde{q}} \left[\frac{4}{27} - \frac{16m_{\tilde{q}}^2}{27\hat{s}} \right] \\
&\quad + \delta_{ij} \frac{\pi \alpha_s \hat{\alpha}_s}{\hat{s}} \left[\beta_{\tilde{q}} \left(\frac{4}{27} + \frac{8m_-^2}{27\hat{s}} \right) + \left(\frac{8m_{\tilde{g}}^2}{27\hat{s}} + \frac{8m_-^4}{27\hat{s}^2} \right) \log \left(\frac{\hat{s} + 2m_-^2 - \hat{s}\beta_{\tilde{q}}}{\hat{s} + 2m_-^2 + \hat{s}\beta_{\tilde{q}}} \right) \right] \\
&\quad + \frac{\pi \hat{\alpha}_s^2}{\hat{s}} \left[\beta_{\tilde{q}} \left(-\frac{4}{9} - \frac{4m_-^4}{9(m_{\tilde{g}}^2 \hat{s} + m_-^4)} \right) + \left(-\frac{4}{9} - \frac{8m_-^2}{9\hat{s}} \right) \log \left(\frac{\hat{s} + 2m_-^2 - \hat{s}\beta_{\tilde{q}}}{\hat{s} + 2m_-^2 + \hat{s}\beta_{\tilde{q}}} \right) \right] \\
\sigma^B(gg \rightarrow \tilde{q} \bar{\tilde{q}}) &= \frac{n_f \pi \alpha_s^2}{\hat{s}} \left[\beta_{\tilde{q}} \left(\frac{5}{24} + \frac{31m_{\tilde{q}}^2}{12\hat{s}} \right) + \left(\frac{4m_{\tilde{q}}^2}{3\hat{s}} + \frac{m_{\tilde{q}}^4}{3\hat{s}^2} \right) \log \left(\frac{1 - \beta_{\tilde{q}}}{1 + \beta_{\tilde{q}}} \right) \right] \\
\sigma^B(q_i q_j \rightarrow \tilde{q} \bar{\tilde{q}}) &= \frac{\pi \hat{\alpha}_s^2}{\hat{s}} \left[\beta_{\tilde{q}} \left(-\frac{4}{9} - \frac{4m_-^4}{9(m_{\tilde{g}}^2 \hat{s} + m_-^4)} \right) + \left(-\frac{4}{9} - \frac{8m_-^2}{9\hat{s}} \right) \log \left(\frac{\hat{s} + 2m_-^2 - \hat{s}\beta_{\tilde{q}}}{\hat{s} + 2m_-^2 + \hat{s}\beta_{\tilde{q}}} \right) \right] \\
&\quad + \delta_{ij} \frac{\pi \hat{\alpha}_s^2}{\hat{s}} \left[\frac{8m_{\tilde{g}}^2}{27(\hat{s} + 2m_-^2)} \log \left(\frac{\hat{s} + 2m_-^2 - \hat{s}\beta_{\tilde{q}}}{\hat{s} + 2m_-^2 + \hat{s}\beta_{\tilde{q}}} \right) \right] \\
\sigma^B(q \bar{q} \rightarrow \tilde{g} \tilde{g}) &= \frac{\pi \alpha_s^2}{\hat{s}} \beta_{\tilde{g}} \left(\frac{8}{9} + \frac{16m_{\tilde{g}}^2}{9\hat{s}} \right) \\
&\quad + \frac{\pi \alpha_s \hat{\alpha}_s}{\hat{s}} \left[\beta_{\tilde{g}} \left(-\frac{4}{3} - \frac{8m_-^2}{3\hat{s}} \right) + \left(\frac{8m_{\tilde{g}}^2}{3\hat{s}} + \frac{8m_-^4}{3\hat{s}^2} \right) \log \left(\frac{\hat{s} - 2m_-^2 - \hat{s}\beta_{\tilde{g}}}{\hat{s} - 2m_-^2 + \hat{s}\beta_{\tilde{g}}} \right) \right] \\
&\quad + \frac{\pi \hat{\alpha}_s^2}{\hat{s}} \left[\beta_{\tilde{g}} \left(\frac{32}{27} + \frac{32m_-^4}{27(m_{\tilde{g}}^2 \hat{s} + m_-^4)} \right) + \left(-\frac{64m_-^2}{27\hat{s}} - \frac{8m_{\tilde{g}}^2}{27(\hat{s} - 2m_-^2)} \right) \log \left(\frac{\hat{s} - 2m_-^2 - \hat{s}\beta_{\tilde{g}}}{\hat{s} - 2m_-^2 + \hat{s}\beta_{\tilde{g}}} \right) \right] \\
\sigma^B(gg \rightarrow \tilde{g} \tilde{g}) &= \frac{\pi \alpha_s^2}{\hat{s}} \left[\beta_{\tilde{g}} \left(-3 - \frac{51m_{\tilde{g}}^2}{4\hat{s}} \right) + \left(-\frac{9}{4} - \frac{9m_{\tilde{g}}^2}{\hat{s}} + \frac{9m_{\tilde{g}}^4}{\hat{s}^2} \right) \log \left(\frac{1 - \beta_{\tilde{g}}}{1 + \beta_{\tilde{g}}} \right) \right] \\
\sigma^B(qg \rightarrow \tilde{q} \tilde{g}) &= \frac{\pi \alpha_s \hat{\alpha}_s}{\hat{s}} \left[\frac{\kappa}{\hat{s}} \left(-\frac{7}{9} - \frac{32m_-^2}{9\hat{s}} \right) + \left(-\frac{8m_-^2}{9\hat{s}} + \frac{2m_{\tilde{q}}^2 m_-^2}{\hat{s}^2} + \frac{8m_-^4}{9\hat{s}^2} \right) \log \left(\frac{\hat{s} - m_-^2 - \kappa}{\hat{s} - m_-^2 + \kappa} \right) \right. \\
&\quad \left. + \left(-1 - \frac{2m_-^2}{\hat{s}} + \frac{2m_{\tilde{q}}^2 m_-^2}{\hat{s}^2} \right) \log \left(\frac{\hat{s} + m_-^2 - \kappa}{\hat{s} + m_-^2 + \kappa} \right) \right],
\end{aligned}$$

with

$$\beta_{\tilde{q}} = \sqrt{1 - \frac{4m_{\tilde{q}}^2}{\hat{s}}} \quad \beta_{\tilde{g}} = \sqrt{1 - \frac{4m_{\tilde{g}}^2}{\hat{s}}} \quad (6)$$

$$m_-^2 = m_{\tilde{g}}^2 - m_{\tilde{q}}^2 \quad \kappa = \sqrt{(\hat{s} - m_{\tilde{g}}^2 - m_{\tilde{q}}^2)^2 - 4m_{\tilde{g}}^2 m_{\tilde{q}}^2} \quad (7)$$

$$\alpha_s = g_s^2 / 4\pi \quad \hat{\alpha}_s = \hat{g}_s^2 / 4\pi. \quad (8)$$

In this paper we set the strong coupling equal to the QCD-SUSY coupling: $g_s = \hat{g}_s$. In our calculation we use the CTEQ6M PDF inside the proton [25]. The factorization and renormalization scales are taken to be $Q = m_{\tilde{q}}, m_{\tilde{g}}$, (the squark and gluino masses respectively). We multiply a K factor of 1.5 to take into account the higher order corrections.

III. SQUARK AND GLUINO PRODUCTION FROM A TEV SCALE BLACK-HOLE AT LHC

If a black hole is formed at LHC, it will quickly evaporate by emitting thermal Hawking radiation. The emission rate in time for a SUSY particle with momentum $p = |\vec{p}|$ and energy $Q = \sqrt{p^2 + M^2}$ can be written [26] as

$$\frac{dN}{dt} = \frac{c_s \sigma_s}{8\pi^2} \frac{dp p^2}{(e^{Q/T_{BH}} \pm 1)} \quad (9)$$

where σ_s is the grey body factor and T_{BH} is the blackhole temperature, which depends on the number of extra dimensions and the TeV scale Planck mass. c_s is the multiplicity factor. The \pm sign refers to squark and gluino respectively. The temperature of the blackhole is given by [6]:

$$T_{BH} = \frac{d+1}{4\pi R_S} = \frac{d+1}{4\sqrt{\pi}} M_P \left[\frac{M_P}{M_{BH}} \frac{d+2}{8\Gamma(\frac{d+3}{2})} \right]^{\frac{1}{1+d}} \quad (10)$$

where R_S is the Schwarzschild radius of the black hole, M_P is the TeV scale Planck mass and d is the number of extra dimensions. The grey body factor in the geometrical approximation is given by [27, 28, 29]

$$\sigma_s = \Gamma_s 4\pi \left(\frac{d+3}{2} \right)^{2/(d+1)} \frac{d+3}{d+1} R_S^2 \quad (11)$$

where we take $\Gamma_s = 2/3$ and $1/4$ for spin $s=1/2$ and 1 particles respectively. The SUSY energy and mass are related by $Q^2 = p^2 + M^2$, where M is the mass of the SUSY particle. From the above equation we get:

$$\frac{dN}{dtdp} = \frac{c_s \sigma_s}{8\pi^2} \frac{p^2}{(e^{\sqrt{p^2+M^2}/T_{BH}} \pm 1)}. \quad (12)$$

The total number of sparticles emitted by a blackhole is thus given by:

$$N_{SUSY} = \int_0^{t_f} dt \int_0^{M_{BH}} dp \frac{c_s \sigma_s}{8\pi^2} \frac{p^2}{(e^{\sqrt{p^2+M^2}/T_{BH}} \pm 1)} \quad (13)$$

where t_f is the total time taken by the blackhole to completely evaporate, a time which takes the form [7]:

$$t_f = \frac{C}{M_P} \left(\frac{M_{BH}}{M_P} \right)^{\frac{d+3}{d+1}} \quad (14)$$

where C depends on the extra dimension, polarization degrees of freedom etc. However, the complete determination of t_f depends on the energy density present out side the blackhole which we computed in a previous paper [18] where we considered the absorption of the

quark-gluon plasma [30] by TeV scale black hole at LHC. (this time is typically about 10^{-27} sec). The value we use throughout this paper is $t_f = 10^{-3}$ fm which is normally the inverse of the TeV scale energy.

This is the expression (Eq. 13) for sparticle emission from a single blackhole of temperature T_{BH} . To obtain the SUSY production cross section from all blackholes produced in pp collisions at LHC we need to multiply the blackhole production cross section with the number of sparticles produced from a single blackhole. In the following we will calculate the blackhole production cross section in a pp collision at LHC. The black hole production cross section σ_{BH} at high energy hadronic collisions at zero impact parameter is given by [6, 17]:

$$\begin{aligned} \sigma_{BH}^{AB \rightarrow BH+X}(M_{BH}) &= \sum_{ab} \int_{\tau}^1 dx_a \int_{\tau/x_a}^1 dx_b f_{a/A}(x_a, Q^2) \\ &\quad f_{b/B}(x_b, Q^2) \hat{\sigma}^{ab \rightarrow BH}(\hat{s}) \delta(x_a x_b - M_{BH}^2/s). \end{aligned} \quad (15)$$

In the above expression $x_a(x_b)$ is the longitudinal momentum fraction of the parton inside the hadron A(B) and $\tau = \frac{M^2}{s}$, where \sqrt{s} is the NN center of mass energy. Energy-momentum conservation implies $\hat{s} = x_a x_b s = M^2$, where M is the mass of the black hole or string ball. We use $Q = M$ as the scale at which the parton distribution function is measured. \sum_{ab} represents the sum over all partonic combinations. The black hole production cross sections in a binary partonic collision are given by [6]

$$\hat{\sigma}^{ab \rightarrow BH}(\hat{s}) = \frac{1}{M_P^2} \left[\frac{M_{BH}}{M_P} \left(\frac{8\Gamma(\frac{d+3}{2})}{d+2} \right) \right]^{2/(d+1)} \quad (16)$$

where M_P and M_{BH} are the Planck mass scale and black hole mass respectively. Again, d denotes the number of extra spatial dimensions. We use the CTEQ6M PDF to compute the blackhole cross section in pp collisions at LHC. The total cross section for SUSY production at LHC is then given by:

$$\sigma_{SUSY} = N_{SUSY} \sigma_{BH}. \quad (17)$$

We now compare this total cross section for SUSY production via black hole resonances with the total number of squarks and gluinos which would be produced via pQCD processes, as explained in section II. To compare the differential cross section we decompose the phase-space integration in eq. (9) as $d^3 \vec{p} = d^2 p_t dp_z = d^2 p_t m_t \cosh y dy$ where $m_t = \sqrt{p_t^2 + m^2}$ and $p^\mu = (m_t \cosh y, p_x, p_y, m_t \sinh y)$.

IV. RESULTS AND DISCUSSIONS

In this section we present the results of our calculation. First of all we present (see Fig. 2) the total blackhole cross section at LHC at $\sqrt{s} = 14$ TeV pp collisions by using eq. (15) with CTEQ6M [25] parton distribution function with factorization scale $Q = M_{BH}$. As black hole mass has to be higher than the Planck mass we have plotted the blackhole cross section for blackhole mass values higher than the Planck mass values. The solid line is for $M_P = 1$ TeV, and the upper (lower) dashed lines are for $M_P = 3$ and 5 TeV respectively. These cross sections are multiplied with the number of SUSY particles emitted from a single blackhole (see eq. (17)) to obtain the total SUSY production cross section at LHC. We have choosen d=4.

In the rest of the calculation we choose following values for the number of extra dimensions, Planck mass and blackhole mass. The number of extra dimension we choose is d=4, the Planck mass $M_P = 1$ (2) TeV with blackhole mass of 3 (5) TeV and the Planck mass $M_P = 3$ TeV with blackhole mass of 5 and 7 TeV and Planck mass $M_P = 5$ TeV with blackhole mass equal to 7 TeV. The typical values (in pico barns) for the cross section for the production of SUSY partners (for example squarks) emitted from a single black hole is around 0.1 to 0.8 depending on the blackhole mass. In Fig. 3 we contrast the result for squark production from the pQCD-SUSY calculation with that from thermal blackhole emission as a function of squark mass in pp collisions at $\sqrt{s} = 14$ TeV at LHC. The solid line is squark production from the pQCD-SUSY calculation with $m_{\tilde{q}}/m_{\tilde{g}}=0.8$. The upper dashed line, lower dashed line and dotted line are squark production from a blackhole at LHC with a number of extra dimensions d=4, Planck mass $M_P = 1$ TeV with blackhole mass equal to 3 TeV, $M_P = 2$ TeV with blackhole mass equal to 5 TeV and $M_P = 3$ TeV with black hole mass equal to 5 TeV respectively. The upper (lower) dot-dashed lines are squark production from a blackhole at LHC with a number of extra dimensions d=4, Planck mass $M_P = 3$ (5) TeV and blackhole mass equal to 7 TeV respectively. It can be seen that the squark production from a TeV scale blackhole with a temperature of about 1 TeV does not depend too much on the squark mass. The pQCD-SUSY result for the production of squarks decreases rapidly as the mass of the squark is increased. On the otherhand, squark production from a black hole is not very sensitive to the squark mass as long as the blackhole temperature is very high. The upper dashed line is for $M_P = 1$ TeV where the blackhole temperature is lower (as the Planck

mass is lower), hence the cross section slightly decreases as the squark mass is increased. All other lines correspond to high temperature (as the Planck mass is increased) and hence the SUSY production cross section is not very sensitive to squark mass. The production cross section of squarks from a blackhole is higher or lower than the pQCD-SUSY production rate for high mass squarks depending on the Planck mass and blackhole mass values. For example if the Planck mass is around 1-3 TeV and black hole mass is around 5 TeV than SUSY production from blackhole is larger for squarks of mass greater than about 300 GeV.

In Fig. 4 we contrast the result for gluino production from the pQCD-SUSY calculation with that from thermal blackhole emission as a function of gluino mass in pp collisions at $\sqrt{s} = 14$ TeV at LHC. The solid line is gluino production from the pQCD-SUSY calculation with $m_{\tilde{q}}/m_{\tilde{g}}=0.8$. The upper dashed line, lower dashed line and dotted line are gluino production from a blackhole at LHC with a number of extra dimensions $d=4$, Planck mass $M_P = 1$ TeV with blackhole mass equal to 3 TeV, $M_P = 2$ TeV with blackhole mass equal to 5 TeV and $M_P = 3$ TeV with black hole mass equal to 5 TeV respectively. The upper (lower) dot-dashed lines are gluino production from a blackhole at LHC with a number of extra dimensions $d=4$, Planck mass $M_P = 3$ (5) TeV and blackhole mass equal to 7 TeV respectively. The pQCD-SUSY result for the production of gluinos decreases rapidly as the mass of the gluino is increased. On the otherhand, gluino production from a black hole is not very sensitive to the gluino mass as long as the blackhole temperature is very high. The upper dashed line is for $M_P = 1$ TeV where the blackhole temperature is lower (as the Planck mass is lower), hence the cross section slightly decreases as the gluino mass is increased. All other lines correspond to high temperature (as the Planck mass is increased) and hence the SUSY production cross section is not very sensitive to gluino mass. The production cross section of gluinos from a blackhole is higher or lower than the pQCD-SUSY production rate for high mass gluinos depending on the Planck mass and blackhole mass values. For example if the Planck mass is around 1-3 TeV and black hole mass is around 5 TeV than SUSY production from blackhole is larger for gluinos of mass greater than about 400 GeV.

In Fig.5 we present the rapidity distribution results for squark production both from pQCD-SUSY processes and from blackholes. The solid line is the squark production cross section from direct pQCD-SUSY production processes as a function of rapidity at LHC at $\sqrt{s} = 14$ TeV pp collisions. Here we have taken $m_{\tilde{q}}/m_{\tilde{g}} = 0.8$. The rapidity range covered is from -3 to 3. The upper (lower) dashed line is the rapidity distribution of squark production

from a blackhole at LHC with a number of extra dimensions d=4, Planck mass $M_P = 2$ (3) TeV and blackhole mass equal to 5 (7) TeV respectively. The production cross section from a blackhole is higher or lower than the pQCD-SUSY production rate for high mass squarks depending on the Planck mass and blackhole mass values. For example if the Planck mass is around 1-3 TeV and black hole mass is around 5 TeV than SUSY production from blackhole is larger for squarks of mass equal to 500 GeV.

Similarly in Fig.6 we present the rapidity distribution results for gluino production, both from pQCD-SUSY processes and from blackholes. The solid line is the gluino production cross section from direct pQCD-SUSY production processes as a function of rapidity at LHC at $\sqrt{s} = 14$ TeV pp collisions. Here we have taken the gluino mass to be 500 GeV with $m_{\tilde{q}}/m_{\tilde{g}} = 0.8$. The rapidity range covered is from -3 to 3. The upper (lower) dashed line is the rapidity distribution of gluino production from a blackhole at LHC with a number of extra dimensions d=4, Planck mass $M_P = 2$ (3) TeV and blackhole mass equal to 5 (7) TeV respectively. The production cross section from a blackhole is higher or lower than the pQCD-SUSY production rate for high mass gluino depending on the Planck mass and blackhole mass values. For example if the Planck mass is around 1-3 TeV and black hole mass is around 5 TeV than SUSY production from blackhole is larger for gluino of mass equal to 500 GeV.

In Fig.7 we present $d\sigma/dp_t$ for the squark production cross section, both from pQCD-SUSY processes and from blackholes. The solid line is the squark production cross section from direct pQCD-SUSY production processes as a function of p_t at LHC at $\sqrt{s} = 14$ TeV pp collisions. Here we have taken the mass to be 500 GeV with $m_{\tilde{q}}/m_{\tilde{g}} = 0.8$. The upper dashed line is the p_t distribution of squark production from a blackhole at LHC with a number of extra dimensions d=4, Planck mass $M_P = 2$ TeV, blackhole mass equal to 5 TeV and squark mass equal to 500 GeV. The lower dashed line is the p_t distribution of squark production from a blackhole at LHC with a number of extra dimensions d=4, Planck mass $M_P = 3$ TeV, blackhole mass equal to 7 TeV and squark mass equal to 500 GeV. The dotted and dot-dashed lines are the similar curves but for squark mass equal to 1 TeV. It can be seen clearly from the figure that $d\sigma/dp_t$ for squark production from a blackhole increases as p_t is increased (in all lines except solid line) up to p_t around 1 TeV (for squark mass equal to 500 GeV) or more (for squark mass equal to 1 TeV) which is in sharp contrast to the pQCD predictions where the $d\sigma/dp_t$ decreases as p_t is increased up to 1 TeV. Similar results are

obtained for gluino production, and this is shown in Fig.8. This increase in $d\sigma/dp_t$ is not only true for SUSY production but also true for any particles emitted from the blackhole as long as the temperature of the blackhole is large (\sim TeV). This is because it is coming from the phase-space (d^3p integration) as at high temperature the decrease of thermal distribution w.r. to p_t is not very rapid. Hence observation of an increase in $d\sigma/dp_t$ (as p_t is increased up to high p_t value ~ 1 TeV or more) for any particles might be a clear signature of black hole production at LHC.

To conclude, if the fundamental Planck scale is near a TeV, then we should expect to see TeV scale black holes at the LHC. Similarly, if the scale of supersymmetry breaking is sufficiently low, then we might expect to see light supersymmetric particles in the next generation of colliders. If the mass of the supersymmetric particle is of order a TeV and is comparable to the temperature of a typical TeV scale black hole, then such sparticles will be copiously produced via Hawking radiation: The black hole will act as a resonance for sparticles, among other things. In this paper we compared various signatures for SUSY production at LHC, and we contrasted the situation where the sparticles are produced directly via parton fusion processes with the situation where they are produced indirectly through black hole resonances. We found that black hole resonances provide a larger source for heavy mass SUSY (squark and gluino) production than the direct pQCD-SUSY production via parton fusion processes depending on the values of the Planck mass and blackhole mass. Hence black hole production at LHC may indirectly act as a dominant channel for SUSY production. We also found that the differential cross section $d\sigma/dp_t$ for SUSY production increases as a function of the p_t (up to p_t equal to about 1 TeV or higher) of the SUSY particles (squarks and gluinos), which is in sharp contrast with the pQCD predictions where the differential cross section $d\sigma/dp_t$ decreases as p_t increases for high p_t about 1 TeV or more. This is a feature for any particle emission from TeV scale blackhole as long as the temperature of the blackhole is very high (\sim TeV). Hence measurement of increase of $d\sigma/dp_t$ with p_t for p_t up to about 1 TeV or more for final state particles might be a useful signature for blackhole production at LHC.

Acknowledgments

We thank Jack Smith, George Sterman, and John Terning for useful discussions. This work was supported in part by the National Science Foundation grant PHY-0098527 and Department of Energy, under contract W-7405-ENG-36.

- [1] N. Arkani-Hamed, S. Dimopoulos and G. Dvali, Phys. Lett. **B429**, 263 (1998); I. Antoniadis, N. Arkani-Hamed, S. Dimopoulos and G. Dvali, Phys. Lett. **B436**, 257 (1998); L. Randall and R. Sundrum, Phys. Rev. Lett. **83**, 3370 (1999); L. Randall and R. Sundrum, Phys. Rev. Lett. **83**, 4690 (1999).
- [2] G. F. Giudice, R. Rattazzi and J. D. Wells, Nucl. Phys. B 544 (1999) 3; L. Vacavant and I. Hinchliffe, J. Phys. G27 (2001) 1839; G. C. Nayak, hep-ph/0211395; Y. A. Kubyshin, hep-ph/0111027; S. B. Bae et al., Phys. Lett. B **487**, 299 (2000); S. C. Park, H. S. Song and J. Song, Phys. Rev. D63 (2001) 077701; K. Cheung, Phys. Rev. D **63**, 056007 (2001).
- [3] W. D. Goldberger and M. B. Wise, Phys. Rev. Lett. **83**, 4922 (1999); Phys. Lett. B **475**, 275 (2000); Phys. Rev. D **60**, 107505 (1999); C. Csáki, M. Graesser, L. Randall and J. Terning, Phys. Rev. D **62**, 045015 (2000); C. Csáki, M. L. Graesser and G. D. Kribs, Phys. Rev. D **63**, 065002 (2001); Phys. Rev. D **62**, 067505 (2000); C. Csaki, J. Erlich and J. Terning, Phys. Rev. D **66**, 064021 (2002); C. Csaki, J. Erlich, T. J. Hollowood and Y. Shirman, Nucl. Phys. B **581**, 309 (2000); E. A. Mirabelli, M. Perelstein and M. E. Peskin, Phys. Rev. Lett. **82**, 2236 (1999); D. Dominici, B. Grzadkowski, J. F. Gunion and M. Toharia, arXiv:hep-ph/0206192; T. Han, G. D. Kribs and B. McElrath, Phys. Rev. D **64**, 076003 (2001); M. Chaichian, A. Datta, K. Huitu and Z. h. Yu, Phys. Lett. B **524**, 161 (2002); J. L. Hewett and T. G. Rizzo, hep-ph/0202155; For a review see G. D. Kribs, hep-ph/0110242.
- [4] A. Chamblin, S. W. Hawking and H. S. Reall, Phys. Rev. **D61**, 065007(2000); R. Emparan, G. T. Horowitz and R. C. Myers, JHEP **0001**, 07(2000); N. Dadhich, R. Maartens, P. Papadopoulos and V. Rezania, Phys. Lett. B487 (2000) 1; A. Chamblin, H. Reall, H. Shinkai and T. Shiromizu, Phys. Rev. **D63**, 064015 (2001); P. Kanti and K. Tamvakis, Phys. Rev. **D65**, 084010 (2002); C. Germani and R. Maartens, Phys. Rev. **D64**, 124010 (2001); I. Giannakis and H. Ren, Phys. Rev. **D63**, 125017 (2001); R. Casadio and L. Mazzacurati, gr-qc/0205129;

P. Kanti, I. Olasagasti and K. Tamvakis, Phys. Rev. D66 (2002) 104026.

[5] T. Banks and W. Fischler, hep-th/9906038.

[6] S. Dimopoulos and G. Landsberg, Phys. Rev. Lett. **87**, 161602 (2001).

[7] S. B. Giddings and S. Thomas, Phys. Rev. D **65**, 056010 (2002).

[8] S. B. Giddings, in *Proc. of the APS/DPF/DPB Summer Study on the Future of Particle Physics (Snowmass 2001)* ed. R. Davidson and C. Quigg, hep-ph/0110127.

[9] D. M. Eardley and S. B. Giddings, Phys. Rev. D66 (2002) 044011.

[10] L. Anchordoqui and H. Goldberg, Phys. Rev. **D65** 047502, 2002.

[11] R. Casadio and B. Harms, Int. J. Mod. Phys. A17 (2002) 4635.

[12] K. Cheung, Phys. Rev. D66 (2002) 036007; K. Cheung, Phys. Rev. Lett. 88 (2002) 221602; K. Cheung and Chung-Hsien Chou, Phys. Rev. D66 (2002) 036008.

[13] Y. Uehara, Mod. Phys. Lett. A17 (2002) 1551.

[14] Seong Chan Park and H.S.Song, hep-ph/0111069.

[15] M. Bleicher, S. Hofmann, S. Hossenfelder, H. Stoecker, Phys. Lett. B548 (2002) 73; S. Hossenfelder, S. Hofmann, M. Bleicher, H. Stoecker, Phys. Rev. D66 (2002) 101502.

[16] I. Mocioiu, Y. Nara and I. Sarcevic, hep-ph/0301073; V. Frolov and D. Stojkovic, gr-qc/0301016; gr-qc/0211055; Phys. Rev. D66 (2002) 084002; D. Ida and S. C. Park, hep-th/0212108; B. Kol, hep-ph/0207037; T. Han, G. D. Kribs and B. McElrath, hep-ph/0207003;

[17] A. Chamblin and G. C. Nayak, Phys. Rev. D66 (2002) 091901.

[18] A. Chamblin, F. Cooper and G. C. Nayak, Phys. Rev. D69 (2004) 065010.

[19] L. A. Anchordoqui, J. L. Feng, H. Goldberg and A. D. Shapere, Phys. Rev. D66 (2002) 103002; J. L. Feng and A. D. Shapere, Phys. Rev. Lett. 88 (2002) 021303; L. A. Anchordoqui, T. Paul, S. Reucroft and J. Swain, hep-ph/0206072.

[20] R. Emparan, M. Masip and R. Rattazzi, Phys. Rev. D65 (2002) 064023.

[21] A. Ringwald and H. Tu, Phys. Lett. B **525**, 135 (2002).

[22] It is worth noting that the string ball picture for the endpoint of Hawking radiation only really makes sense at weak string coupling.

[23] G. Landsberg, Phys. Rev. Lett. 88 (2002) 181801.

[24] W. Beenakker *et al.*, Nucl. Phys. B492 (1997) 51.

[25] J. Pumplin *et al.* J. High Energy Phys. 07 (2002) 012.

- [26] T. Han, G. D. Kribs and B. McElrath, Phys. Rev. Lett. 90 (2003) 031601.
- [27] L. Anchordoqui and H. Goldberg, hep-ph/0209337
- [28] R. Emparan, G. T. Horowitz and R. C. Myers, Phys. Rev. Lett. 85 (2000) 499.
- [29] P. Kanti, J. March-Russell, hep-ph/0212199.
- [30] F. Cooper, E. Mottola and G. C. Nayak, hep-ph/0210391, Phys. Lett. B 555 (2003) 181; G. C. Nayak *et al.*, Nucl. Phys. A687 (2001) 457; R. S. Bhalerao and G. C. Nayak, Phys. Rev. C61 (2000) 054907; G. C. Nayak and V. Ravishankar, Phys. Rev. C58 (1998) 356; Phys. Rev. D55 (1997) 6877.

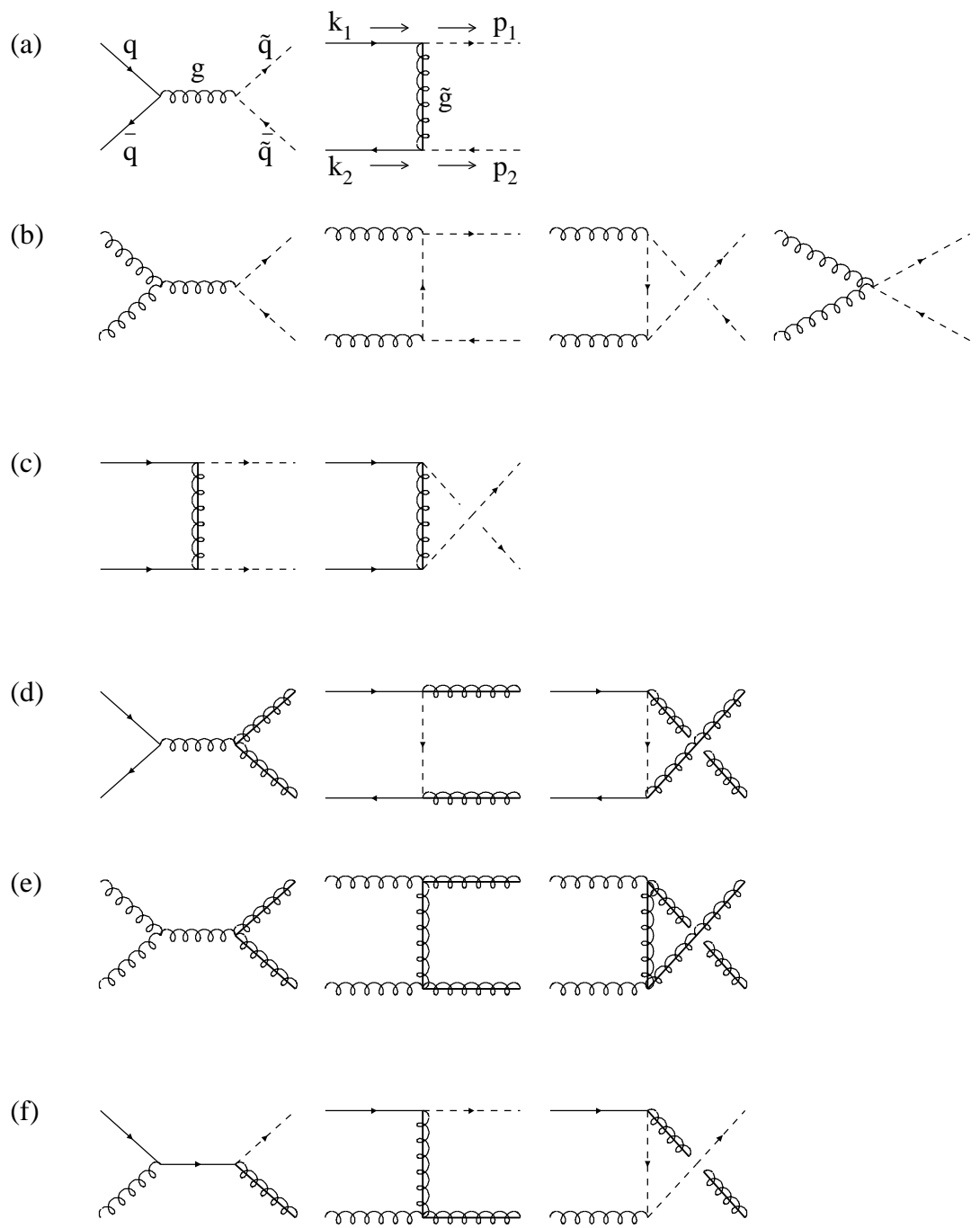


FIG. 1: Feynman diagrams for the production of squarks and gluinos in lowest order.

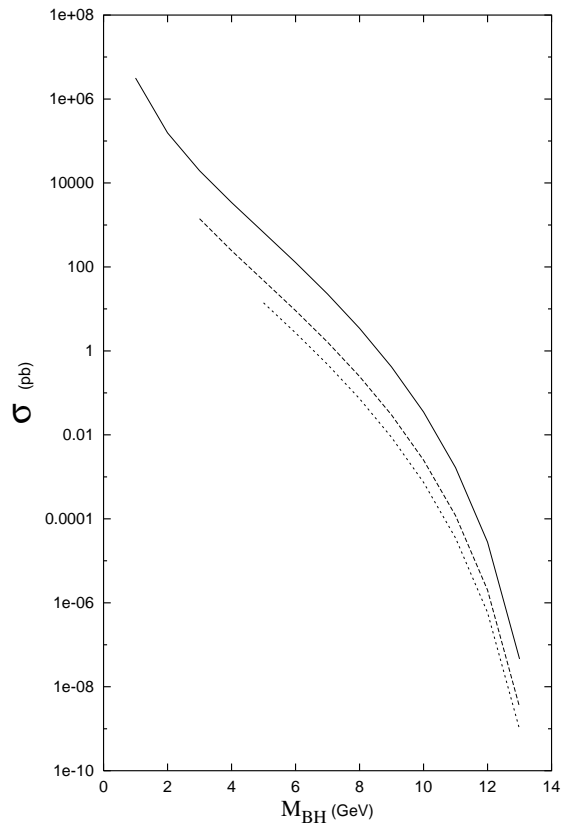


FIG. 2: Total cross section for blackhole production at LHC. The solid line is for $M_P=1$ TeV and the upper (lower) dashed line is for $M_P=3$ (5) TeV.

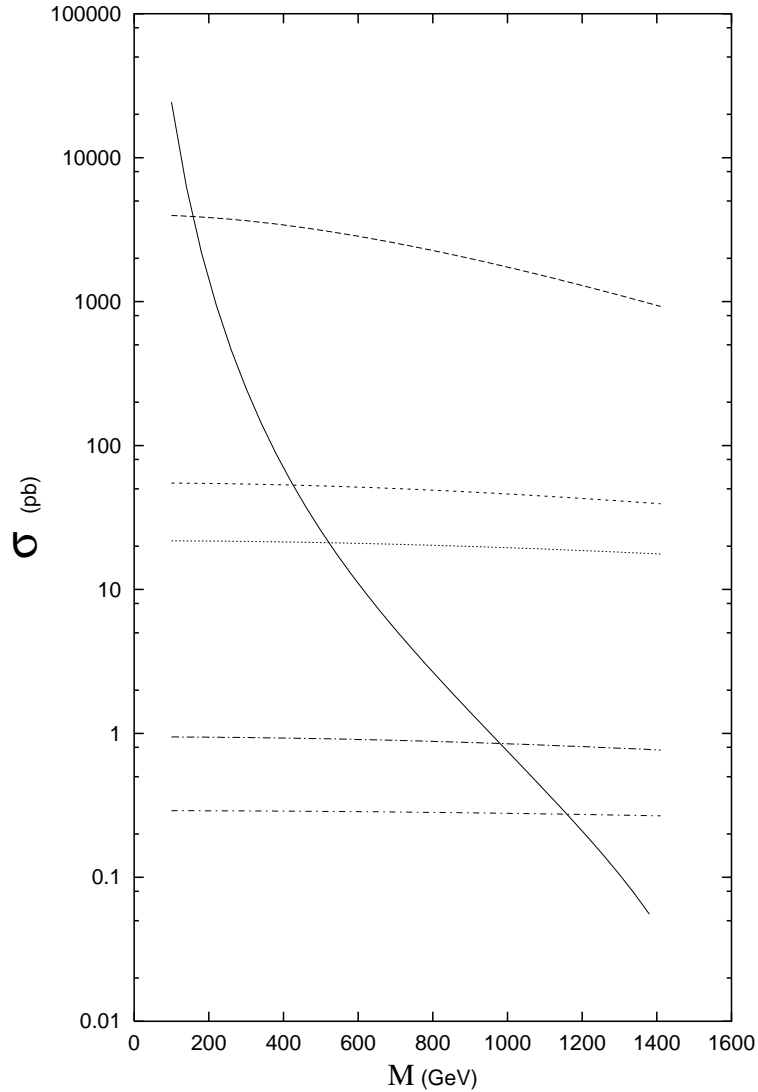


FIG. 3: Total cross section for squark production at LHC as a function of squark mass. The solid line is from direct pQCD processes and other lines are from blackhole decay depending on the Planck mass and blackhole mass as explained in the text. The top line is for blackhole mass equal to 3 TeV, next two almost horizontal lines are for a blackhole mass of 5 TeV and the bottom two are for a blackhole mass of 7 TeV.

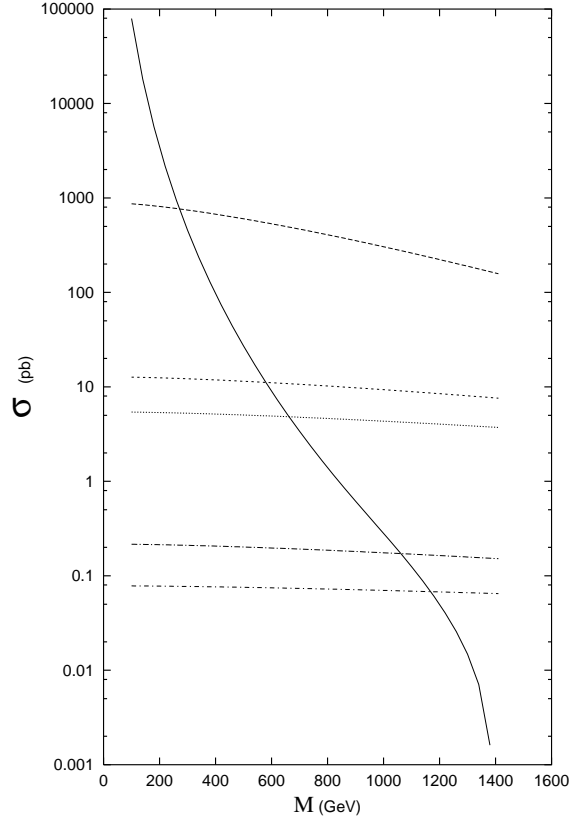


FIG. 4: Total cross section for gluino production at LHC as a function of gluino mass. The solid line is from direct pQCD processes and other lines are from blackhole decay depending on the Planck mass and blackhole mass as explained in the text. Values of the blackhole mass are as in Fig. 3 .

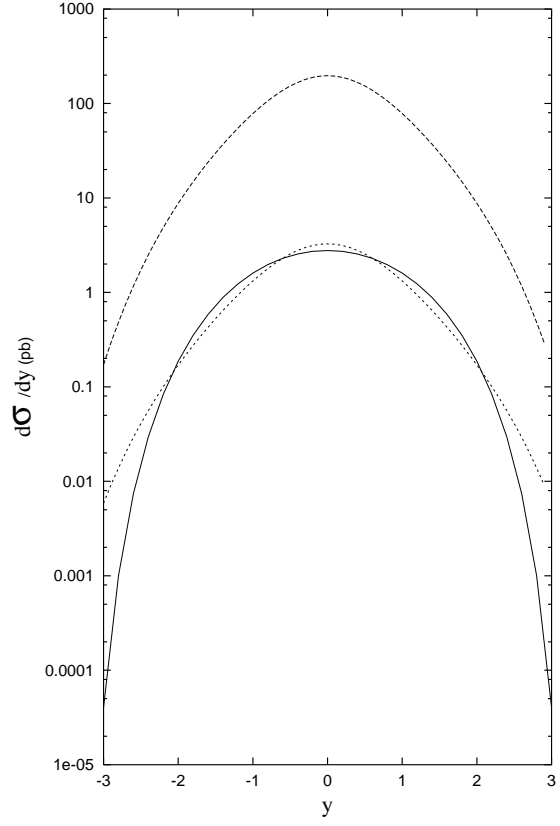


FIG. 5: The rapidity distribution of squark production cross section at LHC. The solid line is from direct pQCD processes and other lines are from blackhole decay depending on the Planck mass and blackhole mass as explained in the text. The squark mass is chosen to be equal to 500 GeV. The upper (lower) dashed line corresponds to a blackhole mass of 5 (7) TeV.

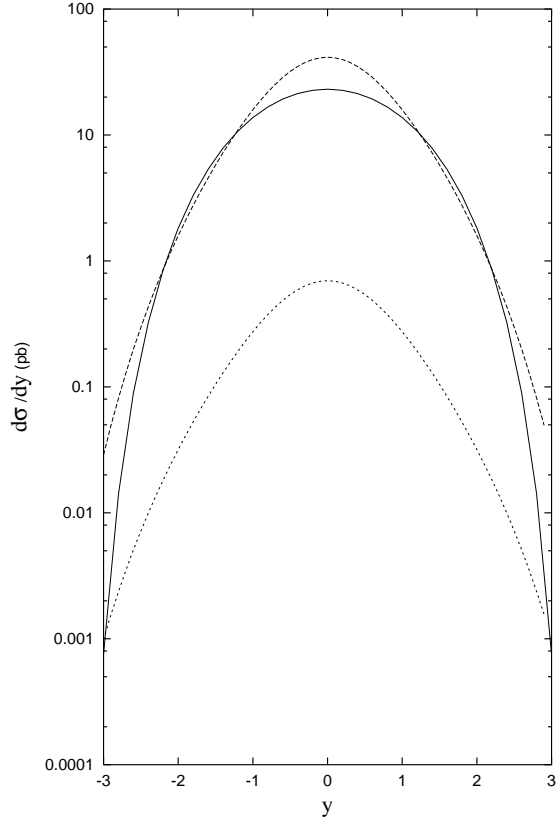


FIG. 6: The rapidity distribution of gluino production cross section at LHC. The solid line is from direct pQCD processes and other lines are from blackhole decay depending on the Planck mass and blackhole mass as explained in the text. The gluino masses are choosen to be equal to 500 GeV. The upper (lower) dashed line corresponds to a blackhole mass of 5 (7) TeV.

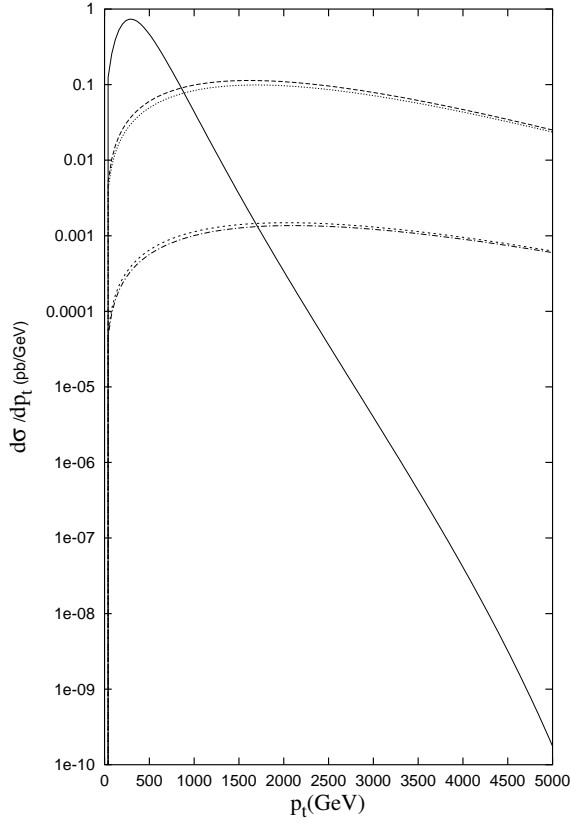


FIG. 7: The p_t distribution of squark production cross section at LHC. The solid line is from direct pQCD processes and other lines are from blackhole decay depending on the Planck mass and blackhole mass as explained in the text. The squark masses are choosen to be equal to 500 GeV and 1 TeV. The upper (lower) other lines correspond to a blackhole mass of 5 (7) TeV.

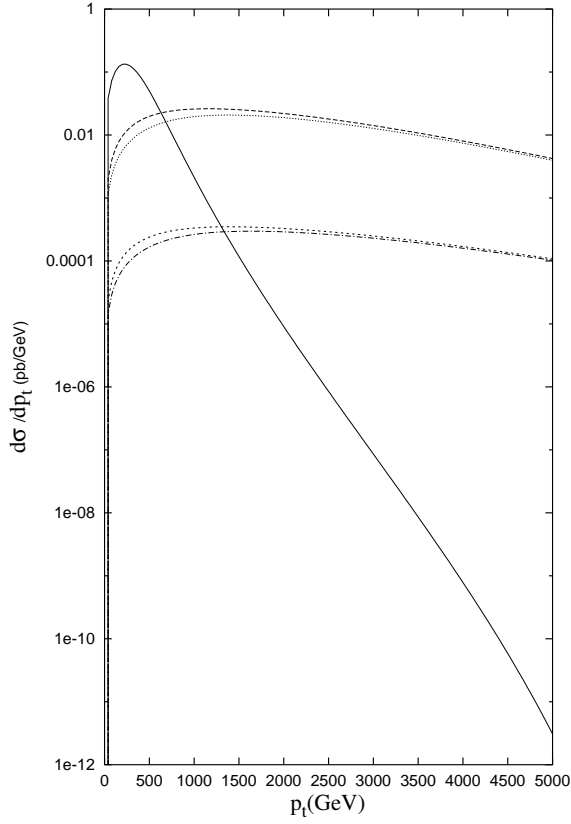


FIG. 8: The p_t distribution of gluino production cross section at LHC. The solid line is from direct pQCD processes and other lines are from blackhole decay depending on the Planck mass and blackhole mass as explained in the text. The gluino mass is choosen to be equal to 500 GeV. The upper (lower) other lines correspond to a blackhole mass of 5 (7) TeV.